Available online at www.sciencedirect.com

ScienceDirect

Energy Procedia 114 (2017) 3219 – 3228

Energy Procedia

13th International Conference on Greenhouse Gas Control Technologies, GHGT-13, 14-18 November 2016, Lausanne, Switzerland

Hydromechanical aspects of CO_2 breakthrough into clay-rich caprock

R.Y. Makhnenko[a,b], V. Vilarrasa[a,c], D. Mylnikov[a], L. Laloui[a]

[a]*Laboratory of Soil Mechanics, École Polytechnique Fédérale de Lausanne, EPFL ENAC IIC LMS, GC – Station 18, CH-1015 Lausanne, Switzerland*

[b]*Department of Civil & Environmental Engineering, University of Illinois at Urbana-Champaign, 205 North Mathews Ave, Urbana, IL, 61801-2352, USA*

[c]*Institute of Environmental Assessment and Water Research, Spanish National Research Council (IDAEA-CSIC), Jordi Girona 18-26, 08034 Barcelona, Spain*

Abstract

Caprock formations are intended to prevent upwards carbon dioxide (CO_2) migration to the surface during CO_2 geological storage. Caprock interaction with CO_2, as well as its potential consequences, requires to be predicted, and thus, need to be studied experimentally. Laboratory investigations of caprock behavior are complex due to its low permeability, and the scarcity of experimental studies involving high-pressure CO_2 injection into caprock representatives puts this difficulty into manifest. In this study, we perform laboratory experiments in an oedometric cell on intact and remolded Opalinus clay (Jurassic shale), evaluating the breakthrough pressure and permeability for liquid and supercritical CO_2. Intact and remolded shale specimens present intrinsic permeabilities of 10^{-21} m^2 to 10^{-20} m^2, respectively. Applied axial stress ranges from 27 MPa to 42 MPa and the pressure and temperature conditions are representative of a caprock at a depth of 800 m. We found that the microstructure of the caprock has a great effect on the material properties. The intrinsic permeability of a more tight material (intact Opalinus clay) is around two times lower than that of remolded shale, which has a more open microstructure. Additionally, the intact rock becomes 30 times less permeable to CO_2 than the remolded shale, which implies that the CO_2 relative permeability is 15 times smaller for intact rock than for remolded shale. On the other hand, CO_2 breakthrough pressure for the tighter material is almost three times lower than for the more permeable remolded shale. Breakthrough pressure of the remolded shale ranges from 3.9 MPa to 5.0 MPa for liquid CO_2 and from 2.8 MPa to 4.6 MPa for supercritical CO_2. For the intact shale, breakthrough pressure is 0.9 MPa for liquid CO_2 and 1.6 MPa for supercritical CO_2. Thus, the breakthrough pressure cannot be correlated with the intrinsic permeability of the caprock.

Peer-review under responsibility of the organizing committee of GHGT-13.

Keywords: Caprock; shale; liquid and supercritical CO_2; breakthrough pressure; permeability.

Peer-review under responsibility of the organizing committee of GHGT-13.

doi:10.1016/j.egypro.2017.03.1453

1. Introduction

The main function of a caprock within carbon dioxide (CO_2) geological storage systems is preventing or minimizing CO_2 leakage to the surface within the timescale of permanent storage projects, i.e., in the order of tens of thousands of years. However, the buoyancy of CO_2, combined with its acidity and potential thermo-mechanical effects, may lead to CO_2 leakage across the caprock. For example, during the first three years of operation at the Sleipner field storage project in the North Sea (Norway), CO_2 propagated upwards through several thin caprock barriers with a total thickness of 17 meters [1]. Furthermore, there are reported cases of naturally accumulated CO_2 invading caprock formations even at relatively small overpressures [e.g., 2, 3]. Since high pressure and large areal extent of CO_2 plumes are expected in industrial scale projects, the risk of CO_2 propagation into the seal increases. In order to plan geological storage projects properly and to perform risk assessment associated with CO_2 propagation through the caprock, the International Energy Agency [4] suggests that each formation should be investigated in terms of its properties (geomechanical and petrophysical) evolution due to interaction with CO_2.

Shales and mudstones are the most typical caprock formations for current and potential CO_2 storage sites due to their low permeability and wide spread in the Earth crust [5]. Existing studies on clay-rich materials' interactions with CO_2 show significant effect of chemical reactions on rock properties and mineral composition [6]. Dissolution of carbonate and feldspar minerals within shales is reported, as well as further secondary carbonate precipitation [7]. While self-sealing caused by CO_2 flow occurs in some occasions due to porosity decrease [e.g., 8] or clogging of fractures [9], other studies show increase of permeability and amount of large pores (> 1 μm) due to interaction with CO_2 [10, 11].

Apart from geochemical reactions, cooling of the lower portion of the caprock may occur [12, 13]. Cooling is likely to be common because injecting CO_2 in liquid state is energetically more efficient than doing so in supercritical state (pressure > 7.382 MPa and T > 31.04 ˚C). It is also more optimal from a storage engineering point of view because liquid CO_2 is denser than supercritical CO_2 [14]. As a result, for a given mass of CO_2, a smaller volume of formation fluid will be displaced leading to a lower overpressure in the reservoir and the increased weight of liquid CO_2 in the injection well implies that a far lower pressure is required at the wellhead. On the other hand, CO_2 will generally reach the storage formation at a colder temperature than that corresponding to the geothermal gradient, because it does not thermally equilibrate with the surrounding rock as it flows downwards along the injection well [15]. The colder CO_2 will form a cooler region around the injection well that advances much behind the desaturation front [12] and that will cool down the caprock by conduction [16]. Moreover, in the case of continuous industrial scale injection, the temperature at which CO_2 enters into the storage formation may be significantly lower than that of the surrounding rock [14, 17]. Hence, strong cooling of the caprock is likely to occur near-the-wellbore and CO_2-caprock interaction should also be studied at temperatures below 31˚C (Fig. 1).

The overarching goal of this study is to identify the main challenges for the caprock integrity (e.g., temperature and chemical effects, long-term permeability, strength evolution) and to study them experimentally for a caprock representative. In this paper, we concentrate on injection of CO_2 inside low-permeable clayey specimens and discuss relative permeability to brine and CO_2 and CO_2 breakthrough pressure. After a brief background section, we introduce the properties of tested materials, experimental setup, and methods, and then provide results, discuss them, and conclude with projections for further studies.

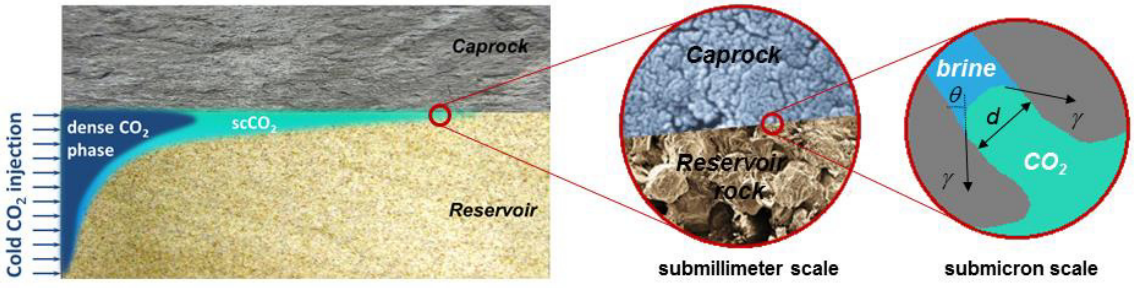

Figure 1. Sketch of CO_2 injection in reservoir rock and its trapping under caprock formation; $scCO_2$ stands for supercritical CO_2.

2. Background

Geomechanical response of a caprock to CO_2 injection involves studying processes that affect elastic and inelastic rock properties and evolution of porosity-permeability relationship [4]. One of the critical parameters for the caprock sealing efficiency is breakthrough pressure, i.e., the excess of CO_2 pressure above initial pore fluid pressure in the caprock that is enough to initiate CO_2 flow through the sealing layer. As a result of CO_2 (non-wetting phase) injection into brine-saturated caprock, its pressure, p_{CO2}, becomes higher than the pressure of brine that initially saturates shale, p_{br}. The difference between the fluid pressure of the non-wetting and wetting phases is the capillary pressure

$$p_{cap} = p_{CO_2} - p_{br}\,. \tag{1}$$

The larger the amount of CO_2 that is injected, the more compressed it becomes and the higher is p_{CO2}. Capillary pressure rises according to (1), until it reaches the gas entry pressure, p_c, and CO_2 enters the caprock pore system. The threshold capillary pressure p_c is an intrinsic property of each particular pore throat, and for an ideal cylinder of diameter d, it is given by the Young-Laplace equation,

$$p_c = \frac{4\gamma\cos\theta}{d}\,, \tag{2}$$

where γ is the surface tension acting at the brine-CO_2 interface and θ is the contact angle of brine-CO_2 surface with respect to the solid phase (Fig. 1). Thus, for a given brine-saturated pore throat of diameter d, CO_2 will enter into it if the CO_2 pressure reaches

$$p_{CO_2} = p_{br} + \frac{4\gamma\cos\theta}{d}\,. \tag{3}$$

A number of studies are dedicated to breakthrough of non-wetting fluids, including CO_2, into shales and other clay-rich materials. The simplest method suggested by IEAGHG [4] involves prediction of the CO_2 entry pressures from the knowledge of corresponding interfacial tensions and contact angles and mercury intrusion porosimetry results for a given caprock. Additionally, the breakthrough pressure can be measured using direct methods, where excess CO_2 pressure is slowly and gradually increased until continuous CO_2 flow is observed [18]. Tanai et al. [19] showed that breakthrough pressures are reproducible, because the pathways created by the first breakthrough experiment are further closed by water imbibition in the absence of fabric damage and become drained again for successive CO_2 breakthrough tests.

Due to the time-consuming nature of direct breakthrough pressure measurements, Hildenbrand et al. [20] and Egermann et al. [21] introduced an indirect experimental technique. They studied a capillary threshold pressure, sometimes referred to as snap-off pressure, and defined the breakthrough pressure as the one at which CO_2 stops flowing through the specimen after its injection is finished. After ceasing the injection, CO_2 upstream pressure starts decreasing due to the resistance of capillary pressure within the pore space, but downstream pressure is maintained constant (see [22] for details). Application of direct and indirect methods gives different breakthrough pressure values for the same material, with variations of 100% and more [23]. Proper explanation of these differences is of great importance because reduction in the breakthrough pressure means reduction in the sealing efficiency of a geological storage system.

Apart from the breakthrough pressure, the effectiveness of a seal is characterized by CO_2 relative permeability. Bocquet and Charlaix [24] demonstrated that the Navier-Stokes equations – and hence Darcy's law – are valid for pore diameters as low as 1 nm, thus are applicable for most of clay-rich materials. An attempt to measure CO_2 relative permeability was performed by Harrington et al. [25], but the low-permeability of shale makes it difficult to interpret the results.

The materials that are considered as potential caprocks for geological storage present permeabilities below 10^{-18} m^2 and high CO_2 entry pressures (~ 1-10 MPa) [26]. The required high-pressure (> 10 MPa) injection tests at elevated temperatures (> 32 ºC) representing in situ conditions and long experimental timescales (~ months) limit laboratory studies. Nevertheless, comprehensive experimental work should allow for proper description of geomechanical and petrophysical properties of clay-rich rocks during CO_2 injection.

3. Experimental methods

3.1. Material

Opalinus clay (shaly facies of Jurassic shale) is a ductile clay-rich (around 60%) material with nano-scale porosity of around 0.12 (Fig. 2), permeability ~ 10^{-20} m^2 [27], and predicted CO_2 entry pressure in the order of a few MPa. Hence, it satisfies the requirements for a potential caprock [26]. In the scope of the current study, two types of fully saturated Opalinus clay specimens are investigated: intact and remolded (i.e., reconstituted) rock. The latter one is assumed to represent material in proximity of faults and fractures within a shale layer [28]. Remolded shale possesses strongly effective mean stress dependent permeability in the range of 10^{-20} – 10^{-18} m^2.

Remolded shale specimens are prepared by crushing the intact material in a grinder and sieving the particles with a size smaller than 0.5 mm. Then, brine corresponding to approximately 1.5 times the liquid limit (or 60%) is added and mixed with the powder. The obtained clay-rich material is consolidated for at least 72 hours in one-dimensional conditions by putting it in the steel-walled tube and applying the axial stress of 350 MPa. The obtained cylindrical specimens have porosity of 0.33 and the degree of saturation of 0.85 - 0.90. Crushing of the clay preserves the flake-like structure of an intact material, but significantly changes the shale properties (e.g., porosity, permeability, bulk moduli) at low effective stresses. However, at the high effective stresses, porosity reduces to 0.15, permeability drops by two orders of magnitude, and bulk modulus increases by a factor of 200, so the material properties appear to be close to those of the intact rock. Additionally, consolidation at high effective stresses makes pore size distribution for remolded shale look similar to the one of intact material (Fig. 2b). In this paper, the remolded shale is referred to as RS, while the intact shale specimen is called OPA.

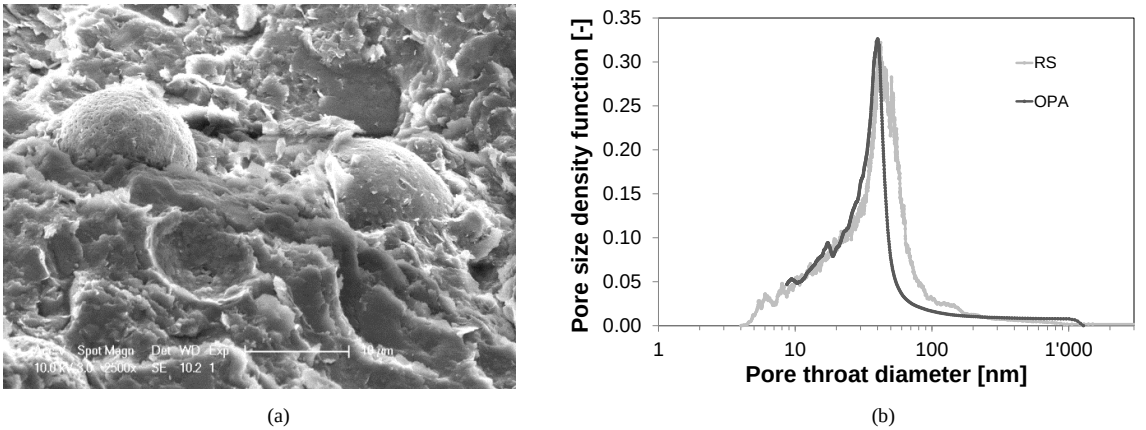

(a) (b)

Figure 2. Unconfined shale specimens: (a) surface electron microscopy of OPA with 2500x magnification and (b) mercury intrusion porosimetry (MIP) test results on OPA and RS.

3.2. Experimental apparatus and technique

Cylindrical specimens (height h = 12.5 mm, diameter D = 35 mm) of remolded and intact shale are prepared and loaded in the oedometric cell, which provides zero lateral strain conditions (Fig. 3). The total mean stress P can be calculated from the generalized Hooke's law knowing the applied vertical stress σ_{ax} and Poisson ratio ν,

$$P = \frac{1+\nu}{3(1-\nu)}\sigma_{ax} \tag{4}$$

The upstream and downstream pressure/volume controllers (GDS Instruments, UK) are utilized to induce pore pressure inside the rock and measure volume of fluid that enters or leaves the specimen. The syringe pump (Teledyne ISCO, USA) is connected in parallel with the upstream pressure/volume controller and is used to inject CO_2 into the sample. The upstream and the downstream pressure lines are instrumented with valves that can prevent the flow and pore pressure transducers providing accurate pore pressure measurements (Fig. 3). In this work, axial

stress was imposed in the range from 27 to 42 MPa, pore fluid pressure – from 8 to 20 MPa, and temperature – at 24 °C and 40 °C. The lower temperature represents near-wellbore case where CO_2 is in liquid state, while imposing the higher temperature allows studying far-from-the-wellbore case with supercritical CO_2. The oedometric cell at the EPFL gives an advantage in studying deformation and fluid flow in low-permeable geomaterials due to relatively small specimen height comparing to conventional triaxial configurations (12.5 mm vs ~ 100 mm). It reduces the experimental time for fluid flow by an order of magnitude and the characteristic diffusion time by two orders of magnitude. All the equipment is placed inside a thermostat room providing constant and well-maintained (within 0.2 °C) temperature during testing and excluding undesirable CO_2 phase transition within the system.

Rock was fully-saturated with the brine having the chemical composition of the formation pore fluid [29] that is supposed to have no chemical effect on the material at in situ conditions. Back pressure saturation method is implemented for ten days with graduate increase of the upstream and downstream pressures and promoting the flow through the specimen. It allows achieving full saturation at brine pressures p > 8 MPa that is confirmed by measurements of constant Skempton's B coefficient values while the effective mean stress (P') is preserved to be constant [30] and equal to 8 MPa. Recorded undrained pore pressure increments are corrected for the influence of "dead" volume [31] and provide B = 0.85 for RS and B = 0.81 for OPA, though the latter one might be affected by the anisotropy of loading. Effective mean stress and bulk moduli are calculated from applied vertical stress and vertical deformation using the following values of drained Poisson ratio ν: 0.30 for RS (at P' < 1 MPa) and 0.33 for OPA (perpendicular to the bedding planes), both measured in conventional triaxial tests.

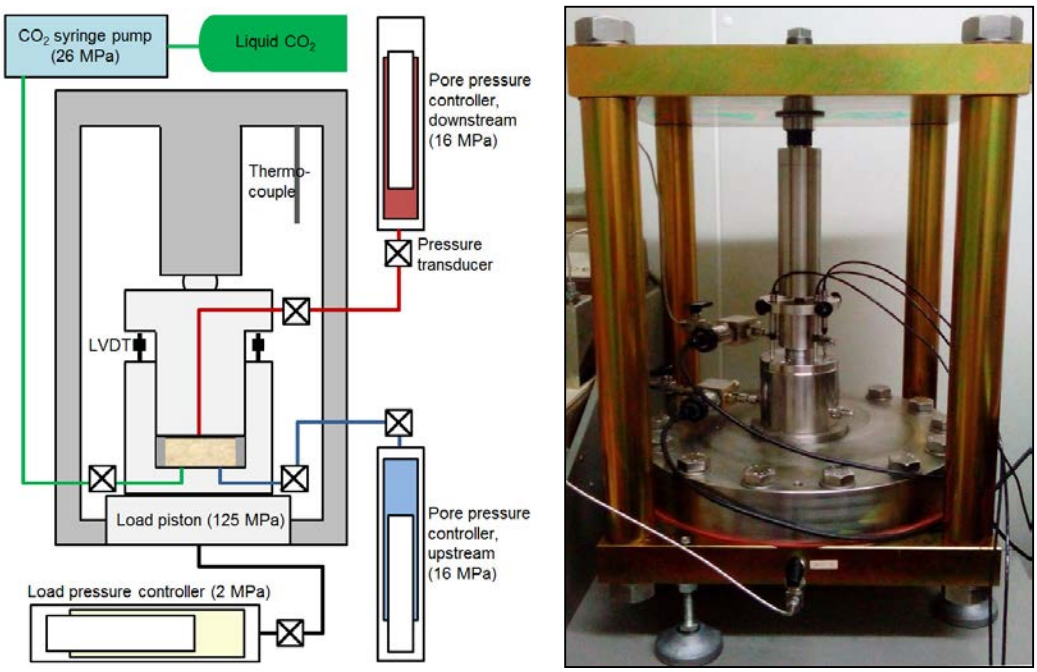

(a) (b)

Figure 3. (a) Schematic diagram and (b) photo of the oedometric loading setup at the EPFL that allows studying flow and mechanical properties of low-permeable rock saturated with brine and high-pressure CO_2.

Intrinsic permeability, k_{int}, is determined from Darcy's law after achieving steady-state flow conditions in the brine saturated specimens

$$k_{int} = -\frac{4\eta_{br} h \Delta V}{\pi D^2 p_{diff} \Delta t}, \quad (5)$$

where η_{br} is brine viscosity (0.001 Pa•s) , p_{diff} is the differential fluid pressure between downstream and upstream of the specimen, and ΔV is fluid volume that passed through the sample during the time period Δt. Considering all the contributing factors, permeability is measured with an accuracy of 2.5% when the duration of steady-state flow exceeds 12 hours. Consistence of measurements is ensured by obtaining constant permeability values with standard deviation of 2.5% for several consecutive measurements at constant differential fluid pressure.

After shale permeability is measured using brine as the only pore fluid, CO_2 is injected into the specimen. Residual pressure technique for the breakthrough pressure measurements [20] is utilized. The downstream pressure/volume controller (Fig. 3) is set to hold the brine pressure at a constant value, 8 MPa in this study. The upstream CO_2 controller is maintaining a pressure that is higher than the downstream brine pressure. It is essential to set p_{diff} larger than the estimated value of CO_2 breakthrough pressure p_{break} to promote CO_2 flow through the rock. The valve within the upstream fluid line is then closed and CO_2 pressure at the upstream side starts decreasing as the flow goes on. As soon as the differential pressure reaches p_{break} value, the reading of the upstream pressure transducer stops decreasing and maintains a constant value. The downstream pressure/volume controller measurements confirm that the fluid flow is blocked by the capillary forces. Measured residual value of p_{diff} is considered as CO_2 breakthrough pressure. In the current study, obtained breakthrough pressure values were confirmed according to the breakthrough definition: CO_2 flow was achieved at p_{diff} being 0.1 MPa higher than p_{break}, while no flow was observed at p_{diff} lower than p_{break}. The accuracy of the breakthrough pressure measurements improves with the increase in the measured p_{break} value, starting from 2% for 0.8 MPa breakthrough pressure.

Following CO_2 breakthrough in the shale, its viscous flow through the material is assumed. The process of steady-state flow is described by Darcy's law with flow in vertical direction only. Darcy's law for the unidirectional case relates the flow rate of the i-th phase $\Delta V_i/\Delta t$ along considered direction to the gradient of differential fluid pressure $p_{diff}/\Delta x$, and can be written in terms of relative permeability of the CO_2 phase k_{rCO2}

$$k_{rCO2} = -\frac{4\Delta V_{CO_2}\eta_{CO_2}h}{k_{int}\pi D^2 p_{diff}\Delta t}, \tag{6}$$

where η_{CO2} is the CO_2 viscosity, which range is $(7.0 – 9.5)\cdot10^{-5}$ Pa•s for liquid CO_2 and $(2.2 – 7.4)\cdot10^{-5}$ Pa•s for supercritical CO_2 at pressures between 8 and 18 MPa [32]. The intrinsic permeability is assumed to remain constant, unless microstructural changes occur inside the specimen. Consistent CO_2 permeability values (within standard deviation of 3%) obtained during several consecutive measurements at constant differential fluid pressure demonstrated relevance of steady-state CO_2 flow assumption.

4. Results

The material properties for remolded and intact shale measured at 27 MPa axial stress and 8 MPa pore pressure, which are representative of storage conditions at 800 m depth, are presented in Table 1. The properties of both materials are very similar, though the remolded shale has a higher porosity, with better interconnected pores than the intact rock, which leads to the permeability increase by almost a factor of two. On the other hand, the geomechanical properties of the two specimens are almost identical.

Table 1: Material properties of intact (OPA) and remolded (RS) shale at σ_{ax} = 27 MPa and p = 8 MPa.

Material	Porosity, n [-]	Permeability, k [m^2]	Bulk modulus, K [GPa]	Skempton's coef., B [-]	Poisson ratio, ν [-]
RS	0.15	$9\cdot10^{-21}$	2.5	0.85	0.30
OPA	0.12	$5\cdot10^{-21}$	2.6	0.81	0.33

Fig. 4a shows residual pressure measurement for RS at 35 MPa axial stress when flowing liquid CO_2 through the sample. Downstream fluid volume indicates when capillary forces block CO_2 flow. The obtained liquid CO_2 breakthrough pressure value of 5.0 MPa is confirmed via the direct method according to the definition of breakthrough (Fig. 4b). Downstream volume measurements in Fig. 4b evidence CO_2 flow at 5.3 MPa differential

pressure, but the flow dramatically decreases at 5.0 MPa differential pressure and completely stops at 4.9 MPa. At this point, all brine in the specimen and connected system is CO_2-rich, because the chemical effect of CO_2 dissolution is much faster than the mechanical effect of breakthrough.

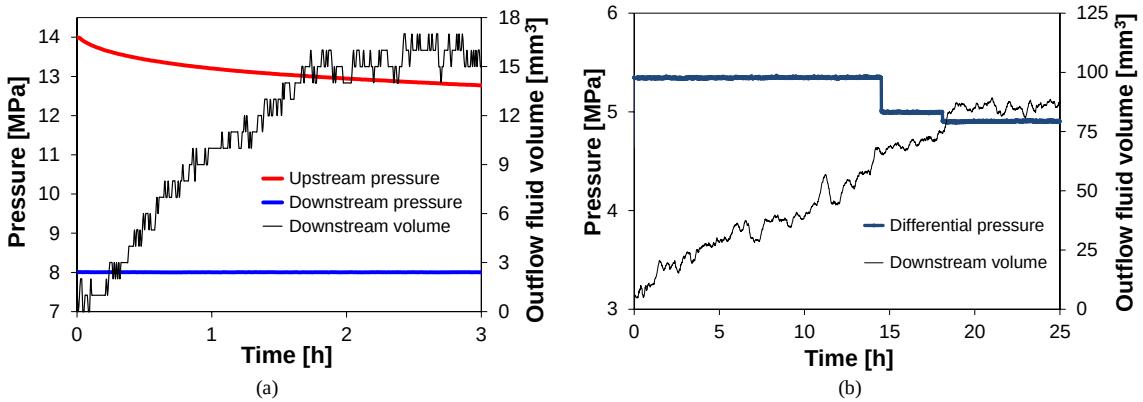

Figure 4. Measurement of liquid CO_2 breakthrough pressure for RS at 35 MPa axial stress. (a) Residual differential pressure is 5.0 MPa, when CO_2 flow stops; (b) confirmation of 5.0 MPa breakthrough pressure: no CO_2 flow at constant differential pressure value of 4.9 MPa.

The breakthrough pressure for liquid and supercritical CO_2 injection are similar regardless of the applied axial stress, except for remolded shale under an axial stress of 35 MPa (Fig. 5). Liquid CO_2 breakthrough pressure is almost 1.8 times higher than that for supercritical CO_2 at 35 MPa. In general, a lower breakthrough pressure is expected for supercritical CO_2 given its lower interfacial surface tension compared to liquid CO_2. However, the observed difference at σ_{ax} = 35 MPa is larger than expected and might be due to a possible heterogeneity generated during the sample preparation of remolded shale.

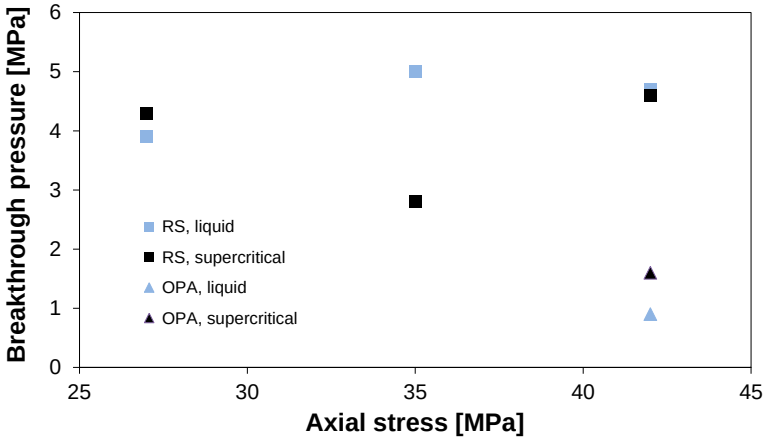

Figure 5. Summary of CO_2 breakthrough pressure measurements: liquid (blue) and supercritical (black) CO_2 in remolded (squares) and intact (triangles) shale specimens.

Fig. 6a shows the CO_2 breakthrough pressure measurements performed on remolded shale at an axial stress of 35 MPa for both liquid and supercritical CO_2. Breakthrough pressure of supercritical CO_2 appears to be lower than that of liquid CO_2 in remolded shale by almost a factor of two: 2.8 MPa vs 5.0 MPa. The low breakthrough pressure of supercritical CO_2 suggests that CO_2 may penetrate into the caprock, at least in regions where, for some reason, the breakthrough pressure is relatively low.

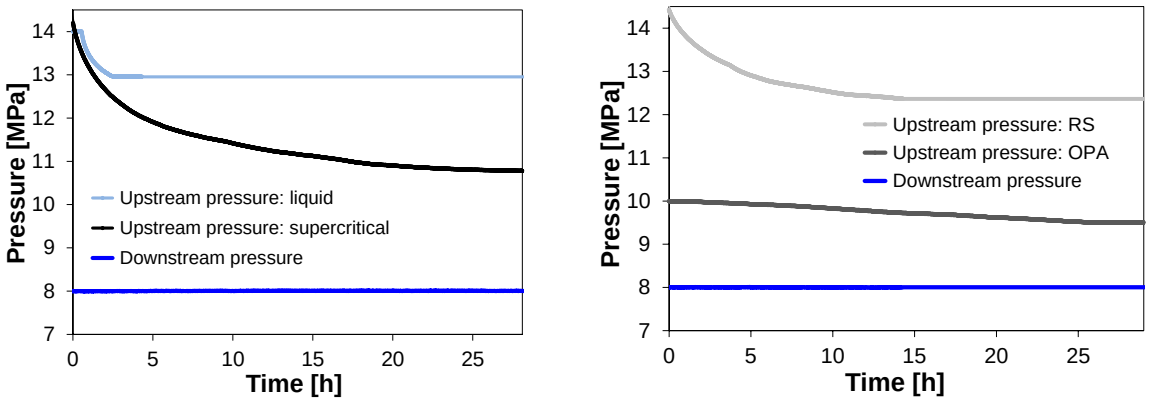

Figure 6. (a) CO_2 breakthrough pressure measurements for remolded shale (RS) at 35 MPa axial stress when flowing supercritical and liquid CO_2; (b) Supercritical CO_2 breakthrough pressure measurements for remolded (RS) and intact (OPA) shale at 42 MPa axial stress.

Unlike RS, intact Opalinus clay specimen (OPA) is not an artificial rock, but a natural caprock representative. CO_2 breakthrough is studied for OPA at an axial stress of 42 MPa. Fig. 6b shows the breakthrough pressure measurements for OPA and RS for CO_2 flow in supercritical state. CO_2 breakthrough pressure turns out to be about three times lower for intact material than for remolded one: 1.6 MPa for OPA and 4.6 MPa for RS, which may be explained by heterogeneity of intact shale specimen where the channels with larger than dominant pore diameter can be found. Further tests are needed to properly assess this observation.

In the case of CO_2 entering into the caprock, the relative permeability to CO_2 would control CO_2 flow across the caprock. CO_2 relative permeability in shale is measured when steady-state flow of CO_2 through the material has been established. The steady-state nature of the flow is ensured once constant permeability values are calculated using equation (6) during several consequent time periods (Fig. 7a). Fig. 7b presents the measurements of the product of the intrinsic permeability and the relative permeability to CO_2 for remolded and intact shale. The only measurement for the intact material – with liquid CO_2 – was conducted at 42 MPa axial stress and resulted in the permeability value 30 times lower than that for the remolded material. Laboratory experiments of CO_2 flow in RS revealed that permeabilities of liquid and supercritical CO_2 are almost identical for remolded shale, both showing a decreasing trend with increasing axial stress. This trend may be related to pore squeezing, which is expected to be a result of axial and, thus, total and effective mean stress increase according to equation (4).

Finally, the saturation of remolded shale with liquid CO_2 is evaluated with the brine imbibition technique. After continuous CO_2 flow is established in the RS specimen at various differential pressures, the upstream channel is closed and brine from the downstream starts replacing CO_2 in the pores. The equilibrium in the system (i.e., constant downstream volume readings) is reached after injection of 140 – 200 mm^3 of brine, which provides the values of 0.10 to 0.14 for CO_2 saturation given that all brine in the system is already CO_2-rich.

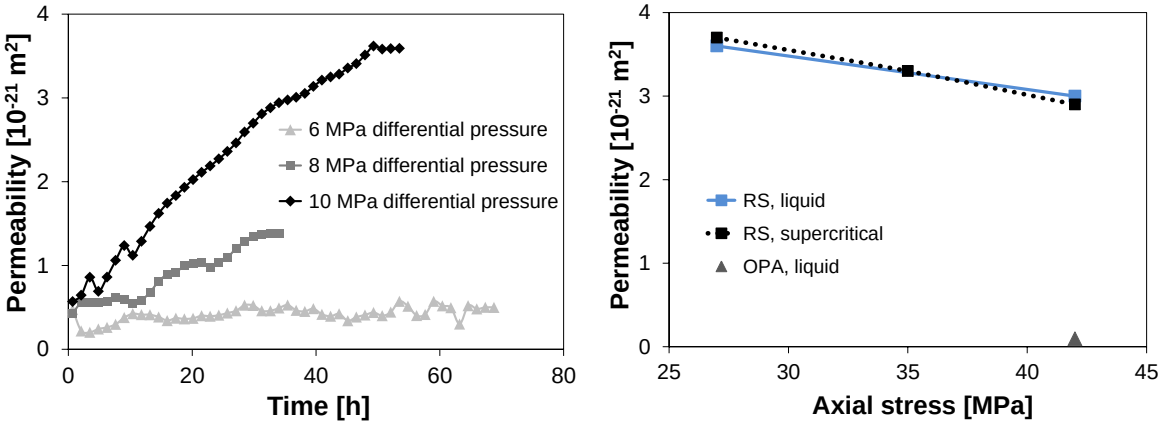

(a) (b)

Figure 7. CO_2 permeability (product of intrinsic permeability and CO_2 relative permeability) for remolded and intact Opalinus clay specimens: (a) time-scale for establishing steady-state flow at various differential pressure values for RS at 27 MPa axial stress; (b) summary of permeability (product of intrinsic permeability and CO_2 relative permeability) measurements for supercritical and liquid CO_2 in RS and OPA at a differential pressure of 10 MPa.

5. Discussion and conclusion

This study highlights the importance of testing shales representative of potential caprocks at realistic conditions that may be encountered in actual CO_2 storage sites. We have tested both remolded and intact Opalinus clay in the oedometric cell at several axial stress values and flowing either liquid or supercritical CO_2. Given fixed pressure and temperature values, most of the tests provided similar (within 5%) values for CO_2 breakthrough pressure measured by two different methods: direct (with the establishment of continuous CO_2 flow) and indirect (through a residual capillary pressure evaluation). From the obtained results, it can be concluded that CO_2 breakthrough pressure and permeability strongly depend on the caprock microstructure and this relationship appears to be of complex nature. This study shows that the intrinsic permeability of a tighter material (intact Opalinus clay) is around two times lower than that of remolded shale, which has a more open microstructure. The pore size has a greater effect on the CO_2 relative permeability, because the intact rock becomes 30 times less permeable to CO_2 than the remolded shale (Fig. 7b). This implies that for a similar CO_2 saturation, the CO_2 relative permeability of intact rock is 15 times smaller than for remolded shale. However, CO_2 breakthrough pressure for the tighter material is almost three times lower than for more permeable material (Figs. 5 and 6b). Thus, the breakthrough pressure cannot be correlated with the intrinsic permeability of the caprock, which is sometimes done in literature [33]. Instead, careful investigation of CO_2 breakthrough and permeability into the caprock has to be conducted, considering various materials under different axial and lateral stresses. Such studies require long experimental times given the low permeability of shales. Although, proper testing as well as the microstructure evolution investigation are necessary to provide the data for improving the fundamental understanding of the phenomena, leading to enhancement in the planning of storage projects.

Acknowledgements

Opalinus clay cores were provided by Swisstopo in the framework of Mont Terri Project, CS-C experiment. R. Makhnenko activities are sponsored by SCCER-SoE (Switzerland) grant KTI.2013.288 and Swiss Federal Office of Energy (SFOE) project CAPROCK #810008154. V. Vilarrasa acknowledges support from the ‘EPFL Fellows’ fellowship programme co-funded by Marie Curie, FP7 Grant agreement no. 291771.

References

[1] Cavanagh AJ, Haszeldine RS. The Sleipner storage site: Capillary flow modeling of a layered CO_2 plume requires fractured shale barriers within the Utsira Formation. International Journal of Greenhouse Gas Control 2014; 21:101-112.

[2] Sorey ML, Evans WC, Kennedy BM, Farrar CD, Hainsworth LJ, Hausback B. Carbon dioxide and helium emissions from a reservoir of magmatic gas beneath Mammoth Mountain, California. Journal of Geophysical Research 1998; 103:15303-15323.

[3] Miocic JM, Gilfillan S, McDermott C, Haszeldine RS. Mechanisms for CO_2 leakage prevention – A global dataset of natural analogues. Energy Procedia 2013; 40:320-328.

[4] IEAGHG. Caprock systems for CO_2 geological storage. IEA Environmental Projects Ltd 2011.

[5] Orr FM Jr. Onshore geologic storage of CO_2. Science 2009; 325:1656-1658.

[6] Song J, Zhang D. Comprehensive review of caprock-sealing mechanisms for geologic carbon sequestration. Environmental Science & Technology 2012; 47(1):9-22.

[7] Liu L, Yu Z, Yang S, Li S, Yang Y. An experimental study of CO_2–brine–rock interaction at in-situ pressure–temperature reservoir conditions. Chemical Geology 2012; 326-327:88-101.

[8] Espinoza DN, Santamarina JC. Clay interaction with liquid and supercritical CO_2: The relevance of electrical and capillary forces. International Journal of Greenhouse Gas Control 2013; 10:351-362.

[9] Noiriel C, Made B, Gouze P. Impact of coating development on the hydraulic and transport properties of argillaceous limestone fractures. Water Resources Research 2007; 43:W09406.

[10] Angeli M, Soldal M, Skurtveit E, Eyvind Aker E. Experimental percolation of supercritical CO_2 through a caprock. Energy Procedia 2013; 1: 3351–3358.

[11] Olabode A, Radonjic M. Shale caprock/acidic brine interaction in underground CO_2 storage. Journal of Energy Resources Technology 2014; 136:042901-1 - 042901-6.

[12] Gor YG, Elliot TR, Prévost JH. Effects of thermal stresses on caprock integrity during CO_2 storage. International Journal of Greenhouse Gas Control 2013; 12:300-309.

[13] Vilarrasa V, Rutqvist J, Rinaldi AP. Thermal and capillary effects on the caprock mechanical stability at In Salah, Algeria. Greenhouse Gases: Science and Technology 2015; 5:449-461.

[14] Vilarrasa V, Olivella S, Carrera J, Rutqvist J. Long term impacts of cold CO_2 injection on the caprock integrity. International Journal of Greenhouse Gas Control 2014; 24:1-13.

[15] Paterson L, Lu M, Connell LD, Ennis-King J. Numerical modeling of pressure and temperature profiles including phase transitions in carbon dioxide wells. In: SPE Annual Technical Conference and Exhibition, 21–24 September 2008, Denver.

[16] Vilarrasa V, Silva O, Carrera J, Olivella S. Liquid CO_2 injection for geological storage in deep saline aquifers. International Journal of Greenhouse Gas Control 2013; 14:84-96.

[17] Garapati N, Randolph JB, Saar MO. Brine displacement by CO_2, energy extraction rates, and lifespan of a CO_2-limited CO_2-Plume Geothermal (CPG) system with a horizontal production well. Geothermics 2015; 55:182-194.

[18] Thomas LK, Katz DL, Tek MR. Threshold pressure phenomena in porous media. SPE Journal 1968; 243:174-184.

[19] Tanai K, Kanno T, Gallé C. Experimental study of gas permeabilities and breakthrough pressures in clays. Materials Research Society Symposium Proceedings 1997; 465:995-1002.

[20] Hildenbrand A, Schlömer S, Krooss BM. Gas breakthrough experiments on fine-grained sedimentary rocks. Geofluids 2002; 2:3-23.

[21] Egermann P, Lombard J-M, Bretonnier P. A fast and accurate method to measure threshold capillary pressure of caprocks under representative conditions. International Symposium of the Society of Core Analysts, Trondheim, Norway; 12–16 September 2006.

[22] Amann-Hildenbrand A, Kroos BM, Bertier P, Busch A. Laboratory testing procedures for CO_2 capillary entry pressures on caprocks. In Gerdes KF (ed.), Carbon Dioxide Capture for Storage in Deep Geological Formations 2015; vol. 4, ch. 25.

[23] Boulin PF, Bretonnier P, Vassil V, Samouillet A, Fleury M, Lombard J-M. Sealing efficiency of caprocks: Experimental investigation of entry pressure measurement methods. Marine and Petroleum Geology 2013; 48:20-30.

[24] Bocquet L, Charlaix E. Nanofluidics, from bulk to interfaces. Chemical Society Reviews 2010; 39:1073–1095.

[25] Harrington JF, Noy DJ, Horsernall ST, Birchall DJ, Chadwick RA. Laboratory study of gas and water flow in the Nordland Shale, Sleipner, North Sea. State of the science: AAPG Studies in Geology 2009; 59:527-543.

[26] IPCC. Special report on carbon dioxide capture and storage. Cambridge University Press 2005.

[27] Bossart P. Characteristics of the Opalinus Clay at Mont Terri. 2012. http://www.mont-terri.ch/internet/montterri/de/home/geology/ key_ characteristics.html

[28] Egholm DL, Clausen OR, Sandiford M, Kristensen MB, Korstgard JA. The mechanics of clay smearing along faults. Geology 2008; 36:787-790.

[29] Pearson FJ. PC experiment: recipe for artificial pore water. Mont Terri Project, Technical Note 2002-17.

[30] ASTM D4767. Standard Test Method for Consolidated Undrained Triaxial Compression Test for Cohesive Soils 2011.

[31] Makhnenko RY, Labuz JF. Elastic and inelastic deformation of fluid-saturated rock. Philosophycal Transactions of Royal Society A 2016; 374:20150422.

[32] Span R, Wagner W. A New Equation of State for Carbon Dioxide Covering the Fluid Region from the Triple-Point Temperature to 1100 K at Pressures up to 800 MPa. Journal of Physical and Chemical Reference Data 1996; 25:1509.

[33] Amann-Hildenbrand A, Bertier P, Busch A, Krooss BM. Experimental investigation of the sealing capacity of generic clay-rich caprocks. International Journal of Greenhouse Gas Control 2013; 19:620-641.